

University of Dundee

Deep learning based defect detection algorithm for solar panels

Li, Jiaqi; Li, Hongxu; Wu, Yifan; Zhou, Hailiang; Manfredi, Luigi; Li, Peng

Published in:
2023 WRC Symposium on Advanced Robotics and Automation (WRC SARA)

DOI:
[10.1109/WRCSARA60131.2023.10261859](https://doi.org/10.1109/WRCSARA60131.2023.10261859)

Publication date:
2023

Document Version
Peer reviewed version

[Link to publication in Discovery Research Portal](#)

Citation for published version (APA):
Li, J., Li, H., Wu, Y., Zhou, H., Manfredi, L., Li, P., & Zhang, H. (2023). Deep learning based defect detection algorithm for solar panels. In *2023 WRC Symposium on Advanced Robotics and Automation (WRC SARA)* (pp. 438-443). IEEE. <https://doi.org/10.1109/WRCSARA60131.2023.10261859>

General rights

Copyright and moral rights for the publications made accessible in Discovery Research Portal are retained by the authors and/or other copyright owners and it is a condition of accessing publications that users recognise and abide by the legal requirements associated with these rights.

- Users may download and print one copy of any publication from Discovery Research Portal for the purpose of private study or research.
- You may not further distribute the material or use it for any profit-making activity or commercial gain.
- You may freely distribute the URL identifying the publication in the public portal.

Take down policy

If you believe that this document breaches copyright please contact us providing details, and we will remove access to the work immediately and investigate your claim.

Deep learning based defect detection algorithm for solar panels

Jiaqi Li¹, Yifan Wu², Hongxu Li³, Hailiang Zhou⁴, Luigi Manfredi⁵ and Hong Zhang⁶

Abstract—Defect detection of solar panels plays an essential phase to guarantee product quality within automated production lines. However, the traditional manual solar panel defects inspection suffers from low efficiency. This paper proposes an enhanced YOLOv5 algorithm (EL-YOLOv5) fuse with the CBAM hybrid attention module to ensure the quality of the product. This algorithm focuses on the detection of five common types of defects that commonly appear on photovoltaic production lines, namely hidden cracks, scratches, broken grids, black spots, and short circuits. This essay utilized publicly available solar panel datasets, as well as datasets collected from actual photovoltaic production lines. These datasets were annotated accordingly, and then using the proposed algorithm to finish the training of two different datasets. The results of the experiments demonstrated that the proposed algorithm achieved good performance on both the public and actual solar panel defect datasets. Especially in actual datasets, defect features are often less apparent, and defects are more minor in size. Nevertheless, the proposed algorithm is still able to detect even minor black spots within these actual datasets.

I. INTRODUCTION

As a safe and environmentally friendly clean energy, solar energy can be converted into electric energy and heat energy, and has broad application prospects. As an important medium for converting solar energy into electrical energy, solar panels are closely related to their production quality and energy conversion efficiency and practical reliability. Therefore, solar panel defect detection is an important link in the automated production line to ensure product quality. Traditional defect detection of the solar panel relies on manual work, which has problems such as high training costs, unstable detection quality, and low detection efficiency. Applying deep learning to defect detection of solar panels can effectively overcome the aforementioned problems.

Object detection is an important branch of computer vision, which can solve both classification and localization problems. The traditional target detection algorithm proposed by Viola-Jones [1] uses the sliding window method for target detection, but the operation speed is relatively slow. HOG [2]

improves detection accuracy and stability through dense grids and contrast normalization, but it is difficult to deal with occlusion problems. DPM [3] is the first traditional target detection algorithm that can adjust the priori frame, but it still has the disadvantages of slow operation speed and low accuracy. The Region based Convolutional Neural Network [4] proposed by Ross Girshick combines the candidate frame with convolution to improve the detection accuracy, but the detection speed is slow. SPPNet [5] extracts features through the feature pyramid, avoids the repeated calculation of the convolution feature map, and improves the detection speed within a limited range. Fast RCNN [6] greatly improves the detection speed by simultaneously training the detector and the bounding box regressor.

In the existing work on defect classification and detection based on deep learning, D. Soukup et al. [7] used photometric stereo images to train the CNN network to classify rail surface defects. Park et al. [8] designed a simple CNN network to automatically detect scratches, burrs and other defects on the surface of parts. Sergiu et al. [9] accomplished solar panel defect classification by deep convolution. Wang et al. [10] aimed at the problems of difficulty in obtaining industrial defect samples and difficult labeling, based on the multi-micrograph convolution (MMGCN) network through label transfer for semi-supervised defect identification and classification of steel surface defects. Xie et al. [11] alleviated the problem of small proportion of defective samples and unbalanced data distribution by separately training CNN models focusing on defective samples and normal samples. Nagata et al. [12] designed a dual-branch CNN network to make full use of the difference between defect samples and normal samples to improve the accuracy of defect classification. The above methods can only classify a single defect sample, but cannot complete the accurate positioning of defects. Cha et al. [13] directly applied Faster R-CNN to bridge surface defect detection, but the detection accuracy was low. Zhong et al. [14] proposed a three-stage defect detection system, but the anchor boxes are too dense and computationally complex, which is not suitable for practical defect detection tasks. Tao et al. [15] designed a two-stage Faster R-CNN network for insulator defect detection through drone inspection, but there is still the problem of slow detection speed, which is not suitable for actual inspection tasks. YOLO [16] has the advantages of simple model, fast detection speed, and high detection accuracy, so it is applied to many practical scenarios. Zhang et al. [17] used YOLOv3 to detect bridge surface defects, introduced pre-trained weights, and further improved the accuracy of defect detection. At the same time, due to the one-stage detection

¹Jiaqi Li is with the Department of Key Lab of Industrial Computer Control Engineering of Hebei Province Yanshan University Qinhuangdao 066004, China. leejq@stumail.ysu.edu.cn

²Yifan Wu is with the Department of Computing Science, University of Alberta, Edmonton, AB T6G 2R3, Canada. ywu35@ualberta.ca

³Hongxu Li is with Automation major of Hebei Province Yanshan University Qinhuangdao 066004, China.

⁴Hailiang Zhou currently serves as a director of Hebei Baoding Jiasheng Photovoltaic Technology Co., Ltd.

⁵Luigi Manfredi is with the Department of Institute for Medical Science and Technology (IMSaT), University of Dundee, United Kingdom. l.manfredi@dundee.ac.uk

⁶Hong Zhang is with the Department of Computing Science, University of Alberta Edmonton, AB T6G 2E8, Canada. hzhang@ualberta.ca

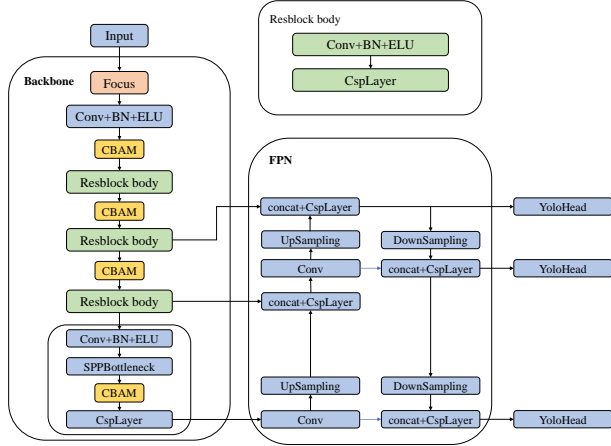


Fig. 1. Network structure of EL-YOLOv5 model

network, the defect detection speed was further improved.

This paper marks the defects in the public solar panel defect data set, and collects the solar panel defect data set on the actual production line, and marks five common types of defects: hidden cracks, scratches, broken grids, black spots, and short circuits. Solar panel defect categories. This paper proposes an improved YOLOv5 [18] algorithm that integrates the mixed attention module of CBAM [19], namely the EL-YOLOv5 detection algorithm. The training results on public datasets and actual solar panel defect datasets show that the proposed algorithm can improve model robustness, convergence speed and detection accuracy.

II. EL-YOLOV5 DETECTION ALGORITHM

A. Network structure

The structure of EL-YOLOv5 Detection Algorithm can be divided into three parts: Backbone, FPN, and Yolo Head. As shown in Figure 1.

(1) Backbone

The backbone of EL-YOLOv5 is its primary feature extraction network[18]. In addition to conventional convolution modules, it includes the Focus, CspLayer, and SPPBottleneck modules as depicted in Figure 2.

The Focus module (Figure a) concentrates width and height information on the channel information, reducing the information loss brought by downsampling. CspLayer (Figure b) saves low-dimensional features and reduces the number of parameters by combining residual stacking and prominent residual edges. SPPBottleneck (Figure c) uses maximum pooling with different kernel sizes for feature extraction, enhancing the network's receptive field.

(2) FPN

FPN serves as an enhanced feature extraction network in EL-YOLOv5, by using semantic and feature information of image characteristics through the fusion of multi-scale

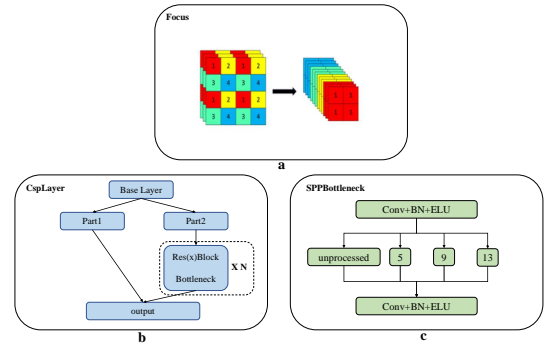


Fig. 2. Sketch maps of Focus, CspLayer and SPPBottleneck

features. This ensures that the model accurately predicts features pertaining to objects of various scales.

(3) YoloHead

The YoloHead comprises Anchors, Convolutional Layers, Prediction Layers, and Non-Maximum Suppression (NMS), which is responsible for multi-scale object detection on the feature maps extracted from the backbone network.

(4) ELU and CBAM

As shown in formula (1) [20], the ELU activation function is continuous and differentiable at all points. As gradients exist for negative values, the issue of dying gradients in the negative region does not occur. Additionally, it is characterized by faster training speed and higher accuracy.

$$ELU(x) = \begin{cases} x & x > 0 \\ a(e^x - 1) & x \leq 0 \end{cases} \quad (1)$$

CBAM, standing for Convolutional Block Attention Module, is a spatial-channel hybrid attention mechanism. As shown in Figure 3, its structure performs weighting on input features in spatial and channel dimensions, enhancing the detection model's ability to focus on significant objects adaptively.

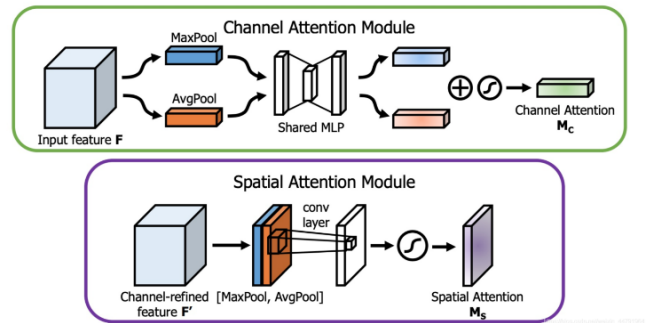


Fig. 3. CBAM attention mechanism

B. Evaluation metrics and loss functions

The evaluation index in this study are divided into quantitative and qualitative indicators. The quantitative indicator is mAP, and the qualitative indicator is the detection result of the model on both public solar panel datasets and actual solar panel datasets.

(1) mAP

The mAP is derived from the model’s precision and recall on the dataset, reflecting the model’s predictive accuracy at different thresholds. The calculation formulas for precision and recall are as shown in formula (2) [21]:

$$\begin{cases} Precision = \frac{TP}{TP+FP} \\ Recall = \frac{TP}{TP+FN} \end{cases}, \quad (2)$$

The curve composed of Precision and Recall is the P-R curve. The area under this curve is the Average Precision (AP). When evaluating the performance across all categories of surface defects on solar panels, the mean of the AP values for each category is mAP.

(2) Loss functions

EL-YOLOv5 includes the following three loss functions: classification loss, localization loss, and confidence loss. The calculation formulas are as follows [18]:

classification loss:

$$y_i = Sigmoid(x_i) = \frac{1}{1 + e^{-x_i}}, \quad (3)$$

$$L_{class} = - \sum_{n=1}^N y_i^* \log(y_i) + (1 - y_i^*) \log(1 - y_i), \quad (4)$$

Note that x_i is the predicted value for the current category, y_i is the class probability for the current category, y_i^* is the actual value for the current category, and L_{class} represents the classification loss.

localization loss:

$$IoU(A, B) = \frac{|A \cap B|}{|A \cup B|}, \quad (5)$$

$$GIoU = IoU - \frac{|C \setminus (A \cup B)|}{|C|}, \quad (6)$$

Note that A is the Ground Truth, B is the Prediction Box, and C is the smallest rectangular box enclosing these two areas. The $GIoU$, compared to the IoU , possesses a Scale-invariant feature, thus yielding higher accuracy.

confidence loss:

The confidence loss is used to adjust the reliability of the predicted bounding box.

Ultimately, the loss function of YOLOv5 consists of a weighted sum of the three types as mentioned earlier of loss, serving as a joint loss function [18]:

$$L = a * L_{class} + b * GIoU + c * L_{con}. \quad (7)$$

III. DATASET PREPARATION

The datasets used in the experiment fall into two categories: publicly available solar panel defect datasets and actual solar panel defect datasets collected in collaboration with photovoltaic companies, both of which were collected using electroluminescent imaging (EL). The format of the defect sample images is JPG, and it includes five common types of solar panel defects: hidden cracks (80), scratches

(66), broken grids (54), black spots (76), and short circuits (62). As shown in Figure 4, the public dataset consists of 691 defect sample images, with 120 hidden cracks, 116 scratches, 108 broken grids, 113 black spots, 114 short circuits, and 120 normal images. The actual dataset consists of 418 images, with 80 hidden cracks, 66 scratches, 54 broken grids, 76 black spots, 62 short circuits, and 80 normal images. The training and testing datasets are divided in a ratio of 6:4, and are all annotated in XML format using Labeling. The Labeling annotation interface is shown in Figure 5.

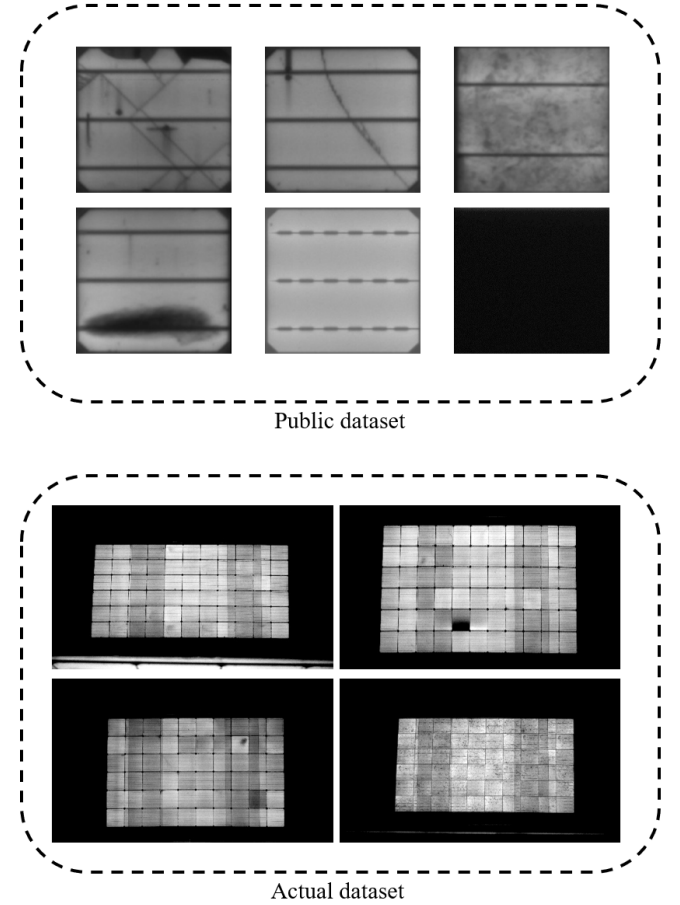


Fig. 4. Solar panel defect dataset



Fig. 5. Annotation interface of Labeling

Finally, annotated solar panel defect samples are stored in

the Annotations folder, the original defect sample images are stored in the *JPEGImages* folder, and all annotated classes are stored in the *predefined_classes.txt* folder. At this point, the annotation of the solar panel defect sample dataset is completed. The annotated class images are shown in Figure 6.

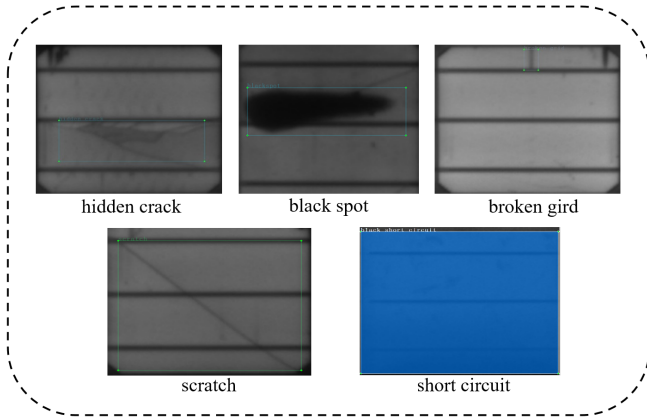


Fig. 6. Annotated images of 5 types of defects

To address the issue that does not have enough sample volume for solar panel, this study enhances and expands the defect sample images through random rotation, slicing, mirroring, and other operations, enriching the data types, and improving the accuracy and robustness of the solar panel defect detection model. The expanded dataset is shown in Figure 7.

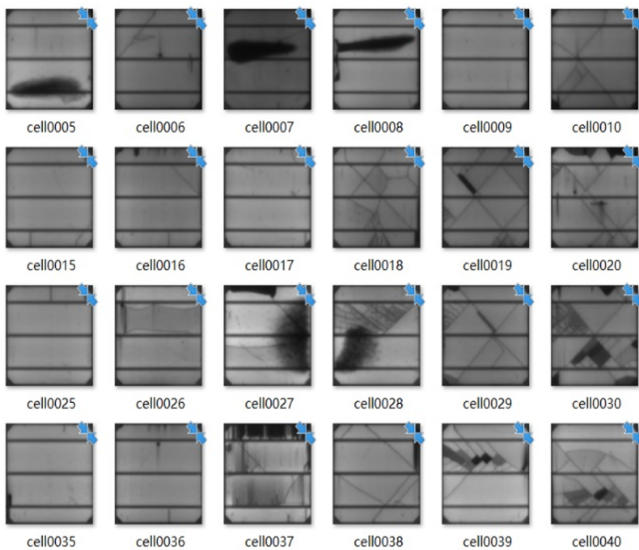


Fig. 7. Expanded sample images (part)

IV. SOLAR PANEL DEFECT DETECTION EXPERIMENT

The EL-YOLOv5 detection algorithm proposed in this paper is based on improvements made to YOLOv5. It is trained and tested on both public and actual solar panel defect datasets and is compared with the pre-improvement YOLOv5 model. While conducting quantitative numerical

TABLE I
EXPERIMENTAL ENVIRONMENT SETTINGS

Project	Version
Programming Language	Python
Framework	PyTorch
Environmental Configuration Tools	Anaconda
Compiler	PyCharm Professional 2022.3
Computer graphics	NVIDIA GeForce GTX 1650
CUDA	12.1
CUDNN	8.9.1
PyTorch	1.12.1

TABLE II
PARAMETER SETTINGS

Parameter	Numerical value
Epochs	300
Batch-size	4
Img-size	640*640
NMS	0.5
Device	GPU

comparisons and curve analysis, we also incorporate intuitive qualitative detection results to demonstrate the effectiveness of the proposed algorithm. The experimental environment settings are shown in Table I.

The experimental parameters used in this study are presented in Table II.

After completing the training of the basic and improved models, the weight files are saved as *best.pt*, which are then called for testing.

A. Quantitative Experiment

The training evaluation metrics in this paper are mAP@0.5 and mAP@0.5:0.95. mAP@0.5 is the mAP when the IOU is set to 0.5, and mAP@0.5:0.95 represents the average mAP at different IOU thresholds (ranging from 0.5 to 0.95, with a step size of 0.05).

The training curves of the traditional YOLOv5 and the improved EL-YOLOv5 detection algorithms on the public solar panel defect dataset are shown in Figure 8.

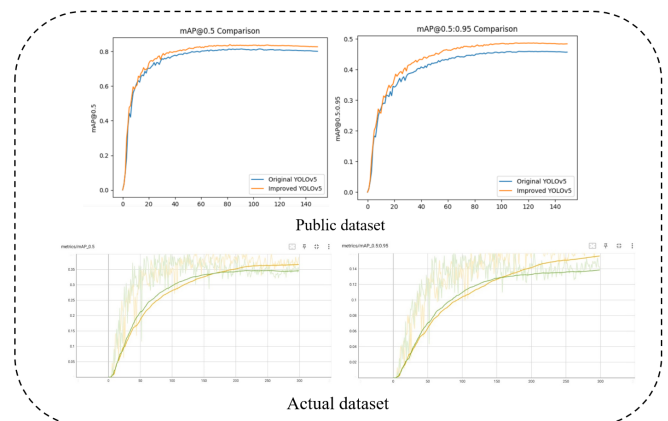


Fig. 8. Training Curves

TABLE III
COMPARISON OF DETECTION ACCURACY

Defect category	Original model	EL-YOLOv5
hidden crack	86%	93%
scratch	84%	92%
broken grid	78%	86%
black spot	85%	95%
short circuit	86%	92%

The public dataset reaches a convergence state after 120 epochs, with a final training accuracy close to 100%. The model converges more slowly and has lower training accuracy on the actual dataset. This is due to insufficient defect samples and high sample complexity under industrial conditions. However, our improved algorithm achieved good training results in both datasets.

The detection accuracy comparison of the traditional YOLOv5 and the solar panel defect detection model improved based on YOLOv5 (EL-YOLOv5) on the public dataset is shown in Table III.

Our algorithm achieved much better detection accuracy in all five categories of solar panel defects.

B. Qualitative Experiment

The detection results of the EL-YOLOv5 detection algorithm on the public and actual solar panel defect datasets are shown in Figure 9.

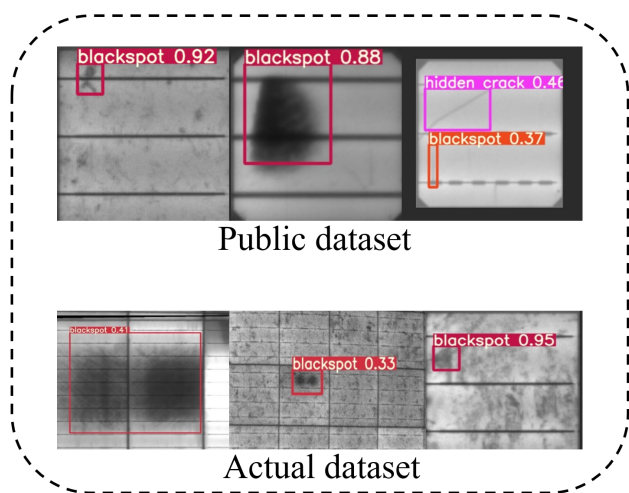


Fig. 9. Defect detection results

As can be seen, the proposed algorithm achieved good results on both the public and actual solar panel defect datasets. Especially, in actual datasets where defect features are often not prominent, and defects are small, our method can still detect minor black spots in the actual dataset.

V. CONCLUSIONS

In response to the issues such as high cost, low detection efficiency, and unstable detection quality inherent in traditional manual inspection of solar panel defects, this paper

introduces the EL-YOLOv5 algorithm for detecting solar panel defects, and applies it to real-life solar panel defect detection on production lines. The paper includes annotations on a publicly available solar panel defect dataset and images of solar panel defects from photovoltaic companies' actual production lines. Addressing the problems of slow training speed and low detection accuracy for minute defects in the conventional YOLOv5, we propose replacing the activation function with ELU and incorporating a mixed attention mechanism in the EL-YOLOv5 detection algorithm, thereby enhancing the model's detection accuracy. Experimental results demonstrate that our proposed algorithm achieves detection accuracies of 93%, 92%, 86%, 95%, and 92% for hidden cracks, scratches, broken grids, black spots, and short circuits, respectively, indicating high accuracy. Qualitative experiments show that our proposed algorithm can not only identify individual defects, but can also distinguish and recognize multiple types of defects. Moreover, it can identify minute black spot defects in the real dataset.

ACKNOWLEDGMENT

The work was partly supported by the Hebei innovation capability improvement plan project (22567619H).

This work was supported by Mr. Zhou Hailiang, a board member of Baoding Jiasheng Photovoltaic Technology Co., Ltd.

REFERENCES

- [1] P. Viola and M. Jones, "Rapid object detection using a boosted cascade of simple features," in *Proceedings of the 2001 IEEE Computer Society Conference on Computer Vision and Pattern Recognition. CVPR 2001*, vol. 1, 2001, pp. 1–I.
- [2] N. Dalal and B. Triggs, "Histograms of oriented gradients for human detection," in *2005 IEEE Computer Society Conference on Computer Vision and Pattern Recognition (CVPR'05)*, vol. 1, 2005, pp. 886–893 vol. 1.
- [3] P. Felzenszwalb, D. McAllester, and D. Ramanan, "A discriminatively trained, multiscale, deformable part model," in *2008 IEEE Conference on Computer Vision and Pattern Recognition*, 2008, pp. 1–8.
- [4] R. Girshick, J. Donahue, T. Darrell, and J. Malik, "Rich feature hierarchies for accurate object detection and semantic segmentation," in *2014 IEEE Conference on Computer Vision and Pattern Recognition*, 2014, pp. 580–587.
- [5] K. He, X. Zhang, S. Ren, and J. Sun, "Spatial pyramid pooling in deep convolutional networks for visual recognition," *IEEE Transactions on Pattern Analysis and Machine Intelligence*, vol. 37, no. 9, pp. 1904–1916, 2015.
- [6] R. Girshick, "Fast r-cnn," in *2015 IEEE International Conference on Computer Vision (ICCV)*, 2015, pp. 1440–1448.
- [7] D. Soukup and R. Huber-Mörk, "Convolutional neural networks for steel surface defect detection from photometric stereo images," 12 2014.
- [8] J.-K. Park, B.-K. Kwon, J.-H. Park, and D. Kang, "Machine learning-based imaging system for surface defect inspection," *International Journal of Precision Engineering and Manufacturing-Green Technology*, vol. 3, pp. 303–310, 07 2016.
- [9] S. Deitsch, V. Christlein, S. Berger, C. Buerhop-Lutz, A. Maier, F. Gallwitz, and C. Riess, "Automatic classification of defective photovoltaic module cells in electroluminescence images," *Solar Energy*, vol. 185, 07 2018.
- [10] Y. Wang, L. Gao, Y. Gao, and X. Li, "A new graph-based semi-supervised method for surface defect classification," *Robotics and Computer-Integrated Manufacturing*, vol. 68, p. 102083, 2021.
- [11] Q. Xie, D. Li, J. Xu, Z. Yu, and J. Wang, "Automatic detection and classification of sewer defects via hierarchical deep learning," *IEEE Transactions on Automation Science and Engineering*, vol. 16, no. 4, pp. 1836–1847, 2019.

- [12] F. Nagata, K. Tokuno, K. Nakashima, A. Otsuka, T. Ikeda, H. Ochi, K. Watanabe, and M. K. Habib, "Fusion method of convolutional neural network and support vector machine for high accuracy anomaly detection," in *2019 IEEE International Conference on Mechatronics and Automation (ICMA)*, 2019, pp. 970–975.
- [13] Y.-J. Cha, W. Choi, G. Suh, S. Mahmoudkhani, and O. Buyukozturk, "Autonomous structural visual inspection using region-based deep learning for detecting multiple damage types," *Computer-Aided Civil and Infrastructure Engineering*, vol. 00, pp. 1–17, 11 2017.
- [14] J. Zhong, Z. Liu, Z. Han, Y. Han, and W. Zhang, "A cnn-based defect inspection method for catenary split pins in high-speed railway," *IEEE Transactions on Instrumentation and Measurement*, vol. 68, no. 8, pp. 2849–2860, 2019.
- [15] X. Tao, D. Zhang, Z. Wang, X. Liu, H. Zhang, and D. Xu, "Detection of power line insulator defects using aerial images analyzed with convolutional neural networks," *IEEE Transactions on Systems, Man, and Cybernetics: Systems*, vol. 50, no. 4, pp. 1486–1498, 2020.
- [16] J. Redmon, S. Divvala, R. Girshick, and A. Farhadi, "You only look once: Unified, real-time object detection," in *2016 IEEE Conference on Computer Vision and Pattern Recognition (CVPR)*, 2016, pp. 779–788.
- [17] C. Zhang, C. Chang, and M. Jamshidi, "Concrete bridge surface damage detection using a singlestage detector," *Comput.-Aided Civ. Infrastruct. Eng.*, vol. 35, no. 4, p. 389409, mar 2020. [Online]. Available: <https://doi.org/10.1111/mice.12500>
- [18] X. Zhu, S. Lyu, X. Wang, and Q. Zhao, "Tph-yolov5: Improved yolov5 based on transformer prediction head for object detection on drone-captured scenarios," in *2021 IEEE/CVF International Conference on Computer Vision Workshops (ICCVW)*, 2021, pp. 2778–2788.
- [19] S. Woo, J. Park, J.-Y. Lee, and I. Kweon, "Cbam: Convolutional block attention module: 15th european conference, munich, germany, september 814, 2018, proceedings, part vii," pp. 3–19, 09 2018.
- [20] D.-A. Clevert, T. Unterthiner, and S. Hochreiter, "Fast and accurate deep network learning by exponential linear units (elus)," *Under Review of ICLR2016 (1997)*, 11 2015.
- [21] T. M. Mitchell, *Machine Learning*, 1st ed. USA: McGraw-Hill, Inc., 1997.